Cellular Signalling 24 (2012) 131–139

Contents lists available at SciVerse ScienceDirect

Cellular Signalling

journal homepage: www.elsevier.com/locate/cellsig

Programmed cell death 6 (PDCD6) inhibits angiogenesis through PI3K/mTOR/p70S6K pathway by interacting of VEGFR-2

Seung Bae Rho [a,*], Yong Jung Song [b], Myong Cheol Lim [b], Seung-Hoon Lee [c], Boh-Ram Kim [a], Sang-Yoon Park [b]

[a] Research Institute, National Cancer Center, 323, Ilsan-ro, Ilsandong-gu, Goyang-si Gyeonggi-do 410–769, Republic of Korea
[b] Center for Uterine Cancer, Research Institute, National Cancer Center, 323, Ilsan-ro, Ilsandong-gu, Goyang-si Gyeonggi-do 410–769, Republic of Korea
[c] Department of Life Science, Yong In University, 470, Samga-dong, Cheoin-gu, Yongin-si Gyeonggi-do 449–714, Republic of Korea

ARTICLE INFO

Article history:
Received 20 April 2011
Received in revised form 2 August 2011
Accepted 20 August 2011
Available online 26 August 2011

Keywords:
Angiogenesis
PI3K/mTOR/p70S6K pathway
Apoptosis
Endothelial cell
Programmed cell death 6

ABSTRACT

Programmed cell death 6 (PDCD6) was originally found as a pro-apoptotic protein, but its molecular mechanism is not well understood. In this study, we have attempted to investigate the effects of PDCD6 on the inhibition of angiogenesis-mediated cell growth as a novel anti-angiogenic protein. Purified recombinant human PDCD6 inhibited cell migration in a concentration–time-dependent manner. We also found that overexpressed PDCD6 suppressed vascular endothelial growth factor (VEGF)-induced proliferation, invasion, and capillary-like structure tube formation in vitro. PDCD6 suppressed phosphorylation of signaling regulators downstream from PI3K, including Akt, mammalian target of rapamycin (mTOR), glycogen synthase kinase-3β(GSK-3β), ribosomal protein S6 kinase (p70S6K), and also decreased cyclin D1 expression. We found binding PDCD6 to VEGFR-2, a key player in the PI3K/mTOR/P70S6K signaling pathway. Taken together, these data suggest that PDCD6 plays a significant role in modulating cellular angiogenesis.

1. Introduction

The 22-kDa calcium-binding protein programmed cell death 6 (PDCD6) was first identified as a pro-apoptotic protein in a genetic screen. PDCD6 contains five EF-hand motifs and an open reading frame encoding 191 amino acids [1]. During the formation of an organism, the balance between cell growth, differentiation, and apoptosis is controlled by a number of regulatory genes. Alterations in this balance are found in diseases such as cancer [2]. The calcium-binding domain of PDCD6 plays a significant role in homodimerization and in the structural changes required for binding to various intracellular protein partners, including Alix [3,4], Fas [5], annexin XI [6], DAPk1 [7], TSG101 [8], Sec31A [9], and PLSCR3 [10].

Several cancer studies have analyzed the mRNA and protein expression of PDCD6 in tissues and cell lines. PDCD6 is ubiquitously expressed in adult mouse tissues but is over-expressed in rat liver hepatoma cells compared to normal liver tissues [11]. PDCD6 expression also appears to be up-regulated in lung cancer patients [11]. In contrast, reduced PDCD6 expression was recently observed in gastric cancer [12]. Hence, we examined whether PDCD6 is generally up-regulated or down-regulated in ovarian tumors. In some cancers, the physiological conditions (e.g., endogenous mRNA and protein levels) in the cancer cells differ from those in normal cells. Our major focus is the regulatory mechanisms of human umbilical vein endothelial cell (HUVEC) and cancer cells. However, we did not investigate the functional role of PDCD6 in angiogenesis further.

In this study, we investigated the detailed functions of PDCD6 during angiogenesis using an in vitro HUVEC system and purified PDCD6. Specifically, we characterized the molecular mechanism of PDCD6 as a novel anti-angiogenic protein. PDCD6 inhibited HUVEC migration in a concentration- and time-dependent manner. In addition, PDCD6 suppressed phosphorylation of signaling components downstream from PI3K, such as Akt, mammalian target of rapamycin (mTOR), glycogen synthase kinase-3β(GSK-3β), ribosomal protein S6 kinase (p70S6K) through direct interactions with VEGFR-2. These interactions significantly control potent anti-angiogenic and anti-tumor activity. Therefore, our results strongly suggest that PDCD6 plays a significant role in modulating cellular angiogenesis.

2. Materials and methods

2.1. Cell lines, tissue samples, cell culture, and antibodies

Primary HUVECs (#CC-2519; Clonetics, San Diego, CA) were cultured on 0.3% gelatin-coated dishes (Sigma, St. Louis, MO) using EGM-2 Bullekit medium (Clonetics). OVCAR-3 ovarian cancer cells were maintained in DMEM medium supplemented with 10% fetal bovine serum (FBS). All

Abbreviations: mTOR, mammalian target of rapamycin; S6K1, ribosomal p70 S6 kinase; MTT, 3-(4,5-dimethylthiazol-2-yl)-2.5-diphenyl-^{2}H-tetrazolium bromide; HUVECs, human umbilical vein endothelial cells; siRNA, small interfering RNA; PDCD6, programmed cell death 6.

* Corresponding author. Tel.: +82 31 920 2383; fax: +82 31 920 2399.
E-mail address: sbrho@ncc.re.kr (S.B. Rho).

0898-6568/$ – see front matter © 2011 Elsevier Inc. All rights reserved.
doi:10.1016/j.cellsig.2011.08.013

cells were maintained under 5% CO_2 at 37 °C. The anticancer agents and chemicals were purchased as follows: rapamycin from Cell Signaling (Beverly, MA); wortmannin and LY294002 from Sigma (St. Louis, MO). The primary antibodies used in this study were anti-PDCD6 (Santa Cruz Biotechnology, Santa Cruz, CA), anti-VEGFR-2 (Santa Cruz), anti-$VEGF_{121}$ (Ab-1; Oncogene, Cambridge, MA), anti-HIF-1α (Santa Cruz), anti-phospho-specific mTOR (Cell Signaling), anti-mTOR (Cell Signaling), anti-PHD2 (Santa Cruz), anti-phospho-specific p38 (Cell Signaling), anti-p38 (Cell Signaling), anti-phospho-specific JNK1/2 (Cell Signaling), anti-JNK 1/2 (Cell Signaling), anti-phospho-specific PI3K (Santa Cruz), anti-PI3K (Santa Cruz), anti-phospho-specific Akt (Santa Cruz), anti-Akt (Santa Cruz), anti-phospho-specific TSC-2 (Santa Cruz), anti-p70S6K (Cell Signaling), anti-phospho-specific GSK-3β (Santa Cruz), anti-cyclin D1 (Santa Cruz), and anti-β-actin (Sigma).

2.2. Preparation of total RNA and RT-PCR analysis of PDCD6 expression

The mRNA expression of *PDCD6* was detected using RT-PCR. Briefly, total RNA was isolated using an RNeasy Mini Kit (Qiagen, Dusseldorf, Germany) according to the manufacturer's instructions and reverse-transcribed using M-MLV reverse transcriptase (Promega, Madison, WI) and random hexamers (Invitrogen, Carlsbad, CA). After cDNA synthesis, PCR was performed using a MyCycler™ Thermal Cycler (Bio-Rad Laboratories Inc., Hercules, CA) with 30 cycles of 1 min at 94 °C, 1 min at 58 °C, and 2 min at 72 °C, followed by a final 10-min extension at 72 °C. The primers used to amplify human *PDCD6* were: 5′-ATGGCCGCCTACTCTTACCG-3′ (sense) and 5′-AGAGGCCAGGGTCATACGATACT-3′ (anti-sense), yielding a 580-bp product. *Glyceraldehyde-3-phosphate dehydrogenase* (*GAPDH*) was used as an internal control in an amount equal to that of the mRNA used. The *GAPDH* primer sequences were: 5′-ATGACCACAGTCCATGCCATC-3′ (sense) and 5′-CCTGCTTCACCACCTTCTTG-3′ (anti-sense), yielding a 271-bp product.

2.3. Purification of recombinant PDCD6 protein

cDNA encoding the full-length of PDCD6 was isolated by RT-PCR described above and introduced into pET29a (Novagen Inc. Madison, WI) using *Eco*RI and *Xho*I. Then construct was expressed in *Escherichia coli* strain BL21 (DE3) grown in Luria Bertani medium supplemented with kanamycin (75 μg/ml). Culture was grown at 37 °C to an $A_{600} = 0.45–0.5$, transferred at 30 °C, and was induced by the addition of 0.4 mM isopropyl-1-thio-β-D-galactopyranoside (IPTG) for 16 h. The induced cells were then harvested and resuspended in 20 mM Tris–HCl (pH 8.0) containing 10% glycerol, 0.1 mM EDTA, 50 mM NaCl, and 1 mM DTT. Cells were lyzed by ultra-sonication, and were centrifuged for 20 min to remove cell debris. The supernatant was filtered and loaded onto a nickel affinity column matrix (Invitrogen) and incubated at 4 °C for 1 h. The slurry was pelleted by centrifugation and washed with washing buffer (20 mM Na_2HPO_4, pH 6.0, 500 mM NaCl) three times. The pellet of the gel matrix was resuspended in elution buffer (20 mM Na_2HPO_4, pH 6.0, 500 mM NaCl containing 400 mM imidazole) and incubated at 4 °C for 20 min to elute the bound His fusion proteins.

2.4. Immunoblotting

Cells and tissues were collected, washed in PBS, and centrifuged. The pellets were then resuspended in cell lysis buffer (50 mM Tris [pH 7.2], 150 mM KCl, 1% Triton X-100, 2 μg/ml aprotinin, 1 mM phenylmethylsulfonyl fluoride, 1 μg/ml leupeptin, and 1 μg/ml pepstatin A) for 30 min. The cell lysates were harvested after centrifugation for 15 min at 12,000×*g*, resolved via SDS gel electrophoresis, transferred to Immobilon P membranes (Millipore Corp., Billerica, MA), and immunoblotted with each antibodies (Santa Cruz) using an ECL detection kit (Amersham Bioscience, Piscataway, NJ). Anti-β-actin antibodies (Santa Cruz) were used as a loading control.

2.5. RNA interference (RNAi)

Small interfering RNA (siRNA) duplex oligonucleotides targeting *PDCD6* (5′-GACAGGAGTGGAGTGATAT-3′) corresponding to nucleotides 212–230 in human *PDCD6* (accession no. NM_013232.3) were prepared using a siRNA expression kit (Ambion, Austin, TX). HUVECs were transfected with the oligonucleotides at a final concentration of 100 nM using Lipofectamine™ Reagent (Invitrogen) according to the manufacturer's protocol. The transfection efficiency of HUVEC and OVCAR-3 cells by using Lipofectamine™ transfection reagent using early passage HUVEC (15–17%) and OVCAR-3 (20–25%) cells were between 15 and 25% in our hands as evidenced by the expression of GFP-tagged-PDCD6 or siPDCD6 expression construct under a fluorescence microscope.

2.6. Cell migration and invasion assay

Cell migration and invasion assays were performed using 8-μm pore-size Transwells (Corning Costar, Cambridge, MA) as described previously [13]. Briefly, HUVECs suspended in DMEM containing 0.1% BSA (Sigma) were seeded onto Matrigel (BD Biosciences, San Jose, CA) in 24-well plates as a monolayer at 3.4×10^4 cells per well. For the migration assays, the lower surface of each filter was coated with 10 μg of gelatin. M199 containing 1% FBS and 25 ng/ml VEGF was placed in the lower chamber, and the cells were allowed to migrate in a 5% CO_2 incubator for 24 h at 37 °C. After incubation, the cells were fixed and stained with hematoxylin and eosin (Sigma) according to the manufacturer's instructions. Nonmigrant cells in the upper chamber were removed by wiping with a cotton swab. Cells that migrated to the lower side of the filter were counted under an inverted microscope, and the mean value of eight fields was determined. For the invasion assay, the lower and upper chambers of the filter were coated with 10 μg of gelatin and 10 μg of Matrigel, respectively. The fixation and quantification methods used were the same as those in the migration assay. Invasive cells were measured from high-power fields.

2.7. Tube formation assay

Growth Factor Reduced Matrigel (200 μl of 10 mg/ml; BD Biosciences) was added to each well of a 24-well plate and incubated at 37 °C for 30 min to allow gel formation. The seeded cells were then incubated with or without 10 ng/ml VEGF for 48 h in M199 containing 1% FBS. Morphological changes were photographed at 40× magnification. Capillary-like tubular structures were observed using an inverted microscope equipped with a digital CCD camera (Zeiss) and quantified using ImageLab imaging software (MCM Design, Copenhagen, Denmark).

2.8. Cell viability assay

Relative rates of cell viability were measured by using MTT assays. Briefly, Cells (C33A, MCF-7, and A549) were seeded at a density of 4.3×10^3–4.7×10^3 cells per well in 96-well plates. Three days after transfection, fresh medium containing 10% FBS and 20 μl of 3-(4,5-dimethylthiazol-2-yl)-2.5-diphenyl-^{2}H-tetrazolium bromide (MTT) solution (Sigma, 5 μg/ml) was added to each well. Each well was then incubated for an additional 4 h at 37 °C. After centrifugation for 10 min at 500×*g*, culture medium supernatant was removed from wells and the formazan was dissolved with DMSO. The amounts of MTT-formazan generated were measured as absorbance using a microplate reader at 570 nm.

2.9. Yeast two-hybrid analysis

For bait construction with human PDCD6, cDNA encoding full-length human PDCD6 was subcloned into the *Eco*RI and *Xho*I restriction enzyme sites of the pLexA cloning vector. The resulting plasmid

pLexA-PDCD6 was introduced into yeast strain EGY48 [*MATa*, *his3*, *trp1*, *ura3-52*, *leu2*::*pLeu2-LexAop6/pSH18-34* (*LexAop-lacZ* reporter)] by a modified lithium acetate method [14]. The human VEGFR-2 was fused by cloning the cDNA fragments into the *Eco*RI and *Xho*I restriction enzyme sites of the pJG4-5 to generate B42 fusion proteins (Clontech, Palo Alto, CA, USA). The cDNAs encoding B42 fusion proteins were introduced into the competent yeast cells that already contained pLexA-PDCD6 and the transformants were selected for the tryptophan prototrophy (plasmid marker) on synthetic medium (Ura, His, Trp) containing 2% (w/v) glucose. The binding activity of the interaction was assayed using an ONPG β-galactosidase assay by the methods of Rho et al. [14].

2.10. Co-immunoprecipitation

To identify the protein interacting partner and targets of PDCD6, gene encoding human PDCD6 was subcloned into pcDNA3.1/Flag (Invitrogen) digested with *Eco*RI and *Xho*I (pcDNA3.1/Flag-PDCD6). The human VEGFR-2 gene was ligated into pcDNA3.1 (Invitrogen) by using *Xho*I (pcDNA3.1-VEGFR-2).

For immunoprecipitation, pcDNA3.1/Flag-PDCD6 and pcDNA3.1-VEGFR-2 expression plasmids were cotransfected into HEK293 cells using Fugene transfection reagent. Lysates were then incubated with anti-Flag antibody (Santa Cruz) and precipitated with protein A-agarose (Amersham). The precipitated proteins were resolved by SDS gel electrophoresis, transferred onto Immobilon P membrane (Millipore corporation), and subjected to immunoblot analysis with anti-PDCD6 or anti-VEGFR-2 antibody.

2.11. Subcloning of deletion mutants of VEGFR-2

Three deletion mutants (Met^{1}-Gly^{800}, Tyr^{801}-Ile^{1180}, Ser^{1181}-Val^{1356}) of VEGFR-2 were isolated by polymerase chain reaction (PCR) using the combination of the following primers (VEGFR-2-F1, 5′-CGGCTCGAGATG-CAGAGCAAGGTGCTG-3′; VEGFR-2-R1, 5′-CGGCTCGAGTCAGCCTGTCTT-CAGTTC-3′; VEGFR-2-F2, 5′-CGGCTCGAGTACTTGTCCATCGTCATG-3′; VEGFR-2-R2, 5′-CGGCTCGAGTCATATCGGAAGAACAAT-3′; VEGFR-2-F3, 5′-CGGCTGGAGTCAGAGACTTTGAGCATG-3′; VEGFR-2-R3, 5′-CGGCTCG-AGTTAAACAGGAGGAGAGCT-3′). PCR products spanning each fragment were cloned into the *Xho*I sites of the pJG4-5. The constructed plasmids were introduced into yeast EGY 48 expressing the pGilda-PDCD6 hybrid protein.

2.12. Luciferase reporter assay

To investigate the VEGFR-2 promoter activity, the VEGFR-2 promoter region was cloned from human placental DNA by PCR using primers (forward primer: 5′-TAGCGAGCTCTGCCACAAGAAGTCCACACA, reverse primer: 5′-CACCCGACCTGTCTGCCTTCC). The fragment containing the VEGFR-2 promoter (from −887 to +295) was eluted from the pCR2.1-TOPO (Invitrogen) vector with *Sac*I and *Xho*I restriction enzymes and was then introduced into the same cloning sites of pGL3 luciferase reporter vector (Promega). The resulting fragments were resolved by 1% agarose gel electrophoresis and performed to confirm correct insert orientation by automatic sequencing (ABI 373, PerkinElmer Life Sciences).

2.13. Statistical analysis

All data were analyzed using Student's *t*-test, followed by a comparison of the mean values of the independent variables. Statistical significance was defined as $P<0.05$.

3. Results

3.1. In vitro inhibition of VEGF-stimulated proliferation and invasion and tube formation by PDCD6

Angiogenesis, the formation of new blood vessels from pre-existing vessels, is an essential step in cancer growth and progression, because it enables the growing cancer to receive oxygen and nutrients. One of the key regulators in vasculogenesis during development is vascular endothelial growth factor (VEGF), which stimulates cell proliferation, differentiation, survival, and migration of endothelial cells. Endothelial cell activity plays an important role in regulating various vascular physiological functions and diseases, including cancer growth and maintenance. Although the detailed analysis on PDCD6 expressions in vesicular endothelial cells during growth and progression has not been done, it has been shown that VEGF or bFGF-induced intracellular calcium signals in endothelial cells reduce angiogenic processes. Thus, we explore the possible function whether PDCD6 modulated the effects of VEGF on cell migration using a modified Boyden Transwell chamber system in HUVECs. Angiogenesis was examined based on cell viability, invasion, and capillary-like tubular structure formation in endothelial cells. The migration of HUVECs treated with various concentrations of purified PDCD6 protein was inhibited in a dose-dependent manner, with the maximum effect at 100 ng/ml (Fig. 1A). To elaborate this finding, we next examined the inhibitory effect of PDCD6 (100 ng/ml) on cell migration over 4, 6, 12, and 24 h (Fig. 1B). After 24 h of treatment with increasing concentrations (0–200 ng/ml) of PDCD6, no migration was detected in the treated samples (data not shown); thus, VEGF-stimulated endothelial cell migration may be specifically inhibited by PDCD6, and not as a side effect of PDCD6 treatment. We also performed more experiments with various concentrations of PDCD6 or siPDCD6 by transient transfection. In Fig. 1C, VEGF enhanced the migration of empty PDCD6-transfected HUVECs when compared with that of un-stimulated cells as expected. However, over-expression of PDCD6 significantly inhibited VEGF-induced migration in a dose-dependent manner. The ablation of over-expressed PDCD6 by siRNA maintained the stimulatory effects of VEGF on migration of HUVECs. Therefore, over-expressed PDCD6 potently inhibited key events of the angiogenic process induced by VEGF, such as migration of endothelial cells in vitro.

To explore the angiostatic effect of PDCD6, we assessed its effect on VEGF-induced endothelial cell proliferation and death. HUVECs were transfected with PDCD6, and cell viability was monitored using a [^{3}H] thymidine incorporation assay. VEGF-stimulated DNA synthesis was assessed in both un-transfected cells and empty mock-transfected cells and compared with that in un-stimulated cells [15]. PDCD6 dramatically reduced cell proliferation to 40–50% that of the control vector (mock), whereas PDCD6 plus siPDCD6 did not inhibit proliferation (Fig. 2A). These results suggest that PDCD6 is a pivotal agent in angiostasis.

To investigate the potential role for PDCD6 up-regulation in inhibiting proliferation and VEGF-mediated angiogenesis, we additionally checked the endogenous levels of PDCD6 in HUVECs. As expected, VEGF increased DNA synthesis (Fig. 2A) as well as protein expression (Fig. 2B, *top*) of empty PDCD6-transfected HUVECs (Mock − treated with VEGF) when compared with un-stimulated cells (indicated as Un or untreated mock). Over-expression of PDCD6 significantly inhibited VEGF-induced protein expression. To further confirm the effect of PDCD6 on endothelial cell proliferation, we used a siRNA (Fig. 2B, *bottom*), which significantly decreased the expression of *PDCD6* mRNA in HUVECs (*lane 2*). However, the siRNA did not affect the expression of the irrelevant gene *GAPDH*. The inhibitory effect of PDCD6 on VEGF-stimulated endothelial cell proliferation was completely rescued by siRNA transiently transfection. These results suggest that VEGF-stimulated endothelial cell proliferation is specifically inhibited by PDCD6.

We also explored the PDCD6-specific inhibition of the VEGF-induced invasion of endothelial cells using Transwell invasion assays. As expected,

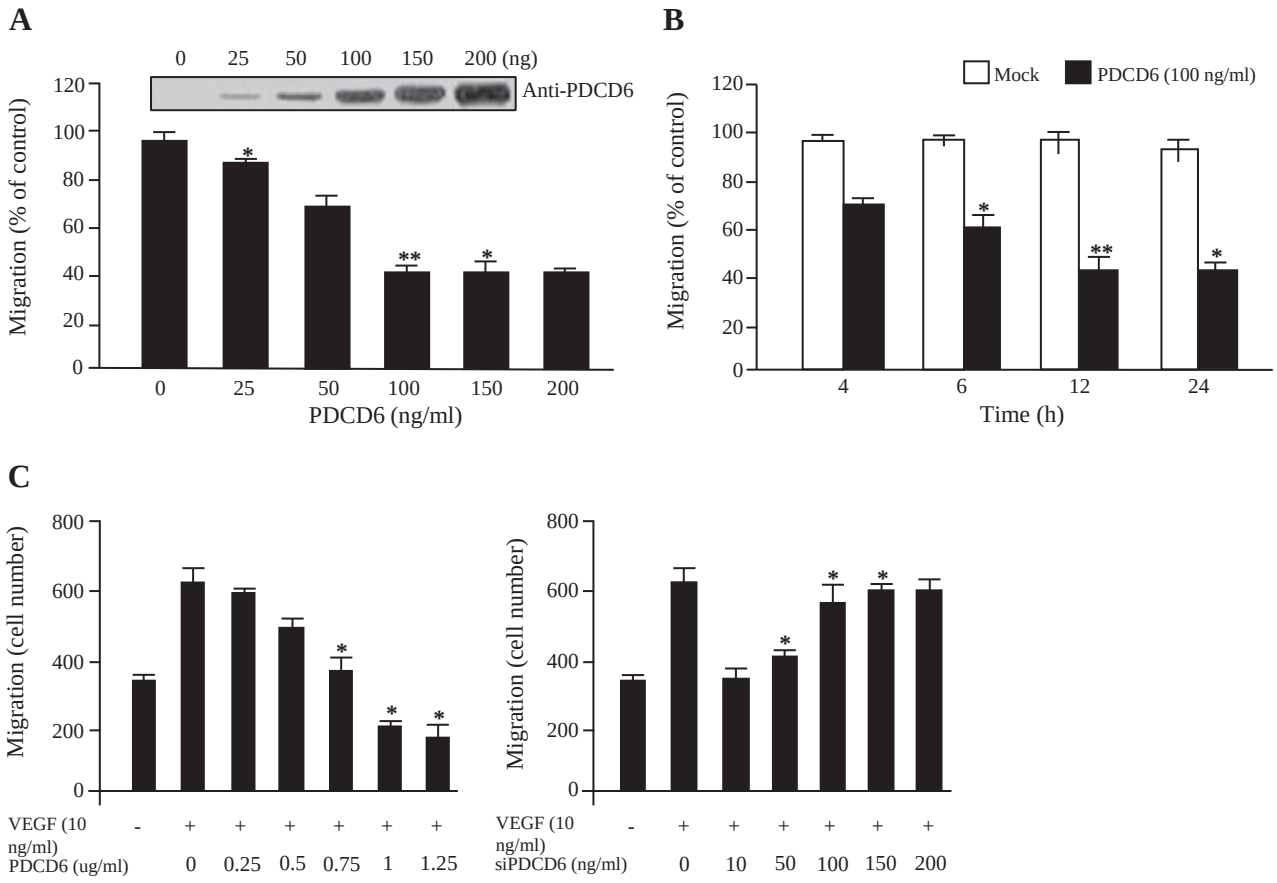

Fig. 1. PDCD6 inhibits VEGF-induced HUVEC migration. (A) HUVECs were cultured on gelatin-coated filters for the migration assay. HUVECs were treated with or without purified PDCD6 protein at different concentrations and incubated for 4 h in Transwell chambers. (B) The percentage of HUVECs that migrated following treatment with purified PDCD6 protein for the indicated times relative to that of mock cells (vector only). (C) After treated with VEGF, HUVECs were transfected with PDCD6 (*left* panel) or siPDCD6 (*light* panel) construct at different concentrations. The number of migrated cells was determined under a light microscope and is indicated as the mean ± SD. The results shown are representative of at least three independent experiments. *, $P<0.05$ and **, $P<0.01$.

VEGF increased the invasion of untransfected cells and empty mock-transfected cells compared with that of unstimulated cells. Our results indicate that PDCD6 over-expression significantly blocked VEGF-stimulated cell invasion while PDCD6-siRNA did not (Fig. 2C). Thus, over-expressed PDCD6 inhibits key events in VEGF-induced angiogenesis in vitro, including endothelial cell proliferation, migration, and invasion.

Finally, we assessed the anti-angiogenic effects of PDCD6 on VEGF-induced tube formation using an in vitro angiogenesis model involving capillary-like tubule formation in HUVECs on Matrigel. As shown in Fig. 2D, untreated or control cells incubated with VEGF formed a capillary-like structure on Matrigel. In contrast, the ectopic expression of PDCD6 completely inhibited VEGF-stimulated tubular structure formation. The inhibitory effect of PDCD6 on VEGF-stimulated tube formation was completely rescued by siRNA transfection. Taken together, these findings indicate that PDCD6 specifically modulates VEGF-induced HUVEC invasion and tube formation.

3.2. PDCD6 inhibits PI3K activation and Akt (Ser-473) phosphorylation

VEGF stimulates angiogenesis in tumorigenesis and tumors; hence, we examined the inhibitory effect of PDCD6 on VEGF expression in OVCAR-3 ovarian cancer cells. The ectopic expression of PDCD6 completely inhibited VEGF expression, whereas siPDCD6 had no effect (Fig. 3A). We also investigated the effect of PDCD6 on HIF-1α expression. HIF-1α is an important element for VEGF expression as a transcription factor. As shown in Fig. 3A, PDCD6 markedly decreased the expression of HIF-1α protein. The inhibitory effect of PDCD6 was completely restored by siRNA transfection. These observations indicate that VEGF-induced protein expression is specifically suppressed by PDCD6.

PI3K/Akt phosphorylation is a critical step in tumor growth and angiogenesis, and Akt plays a pivotal role as a downstream target of PI3K. Akt is promoted by several growth factors and enhances cell survival; therefore, we examined whether PDCD6 inhibited PI3K and Akt phosphorylation in OVCAR-3 cells. Cell lysates from control and treated cells were subjected to immunoblot analysis, which showed that the VEGF-induced phosphorylation of PI3K and Akt plays a fundamental role in VEGF-induced angiogenesis. As shown in Fig. 3B–C, VEGF-stimulated PI3K and Akt phosphorylation was markedly inhibited by PDCD6. These results were comparable to that of wortmannin and LY294002, which are well-known PI3K inhibitors. Wortmannin and LY294002 had shown a 10–15% lower activity than that of PDCD6 (Fig. 3B). We also investigated the effects of rapamycin, a well-known specific inhibitor of mTOR signaling pathway. As presented in Fig. 3D, PDCD6 and wortmannin treatment inhibited Akt phosphorylation, but rapamycin did not affect the expression of Akt phosphorylation. These findings strongly suggest that PDCD6 can suppress cell proliferation through inhibiting PI3K/Akt phosphorylation.

The normal (HUVEC) and cancer (OVCAR-3) cells are different in terms of their biological/physiological conditions including endogenously mRNA and protein levels. Our major concern is about the regulation mechanism in cancer cells. To further confirm the functional effect of PDCD6 with a variety cancer cell lines, C33A (cervical), MCF-7 (breast), and A549 (lung) cells were transfected with mock (an expression vector only without insert), PDCD6 or PDCD6 plus

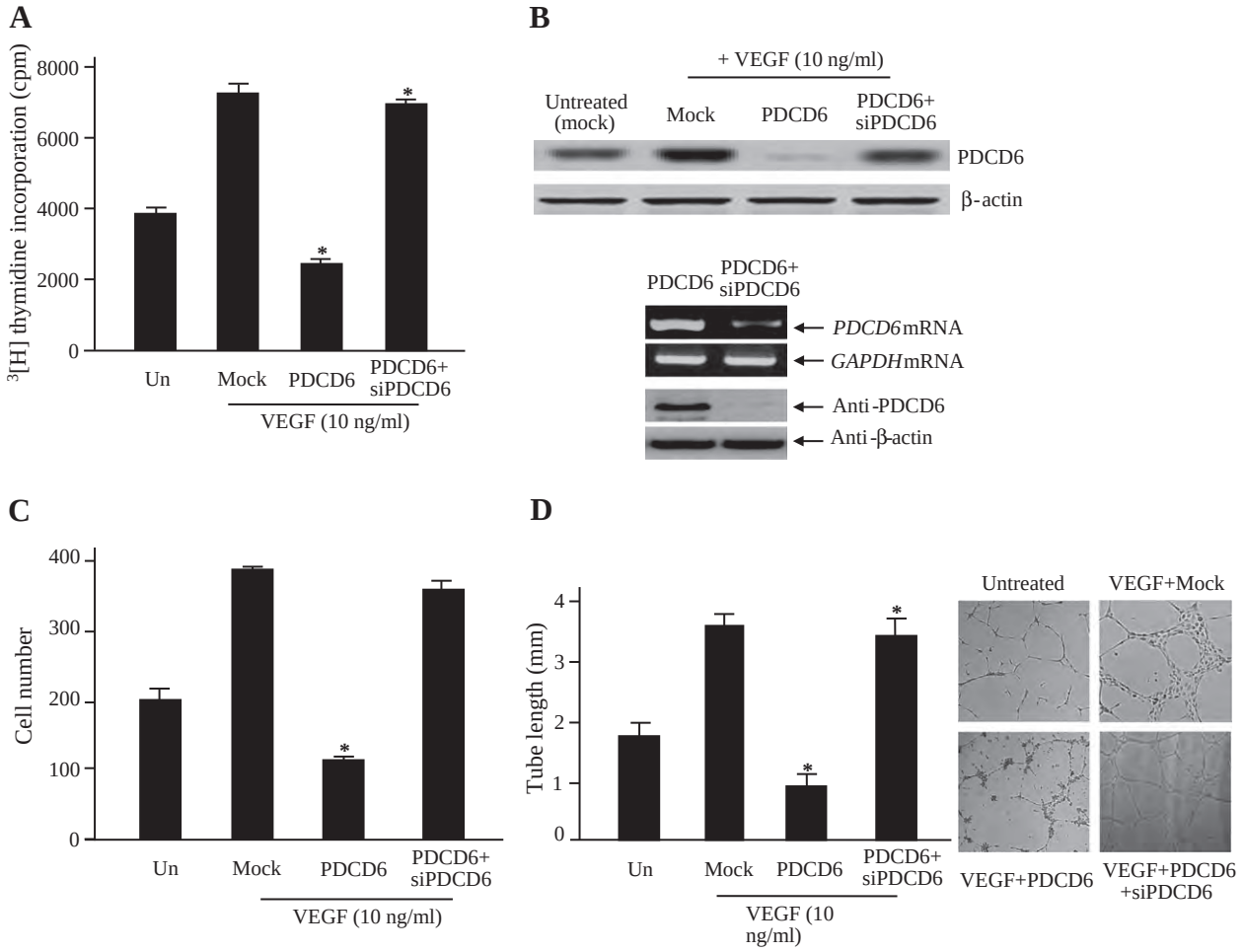

Fig. 2. In vitro PDCD6 inhibition of angiogenic activity in HUVECs. (A) The growth inhibitory effect of human PDCD6 on HUVEC proliferation. Each transfectant was seeded for 3 days in the presence of VEGF. The c.p.m. value of [^{3}H]thymidine was measured using a liquid scintillation counter. The data are the means ± SDs of three separate experiments. (B) Inhibition of VEGF-mediated angiogenesis by PDCD6 in HUVECs. After treated with VEGF, HUVECs were transfected with Flag-fused PDCD6 cDNA alone (Flag-PDCD6) or co-transfected with Flag-fused PDCD6 cDNA and siRNA (Flag-PDCD6 + siRNA). Untreated mock is the levels of endogenous PDCD6 in HUVECs (*top* panel). Elimination of Flag-fused protein and mRNA expression by siRNA in HUVECs. After transfection, the cells were observed under a fluorescence microscope and the mRNA or protein expression levels were investigated using RT-PCR and Western blotting (*bottom* panel). *GAPDH* and β-actin were used as mRNA and protein loading controls, respectively. (C) Effect of human PDCD6 on HUVEC invasion. Transfectants were examined using Matrigel-coated Transwells for invasion assays, followed by induction for 48 h in the absence or presence of VEGF. The number of cells that invaded was counted under a light microscope, and the mean values were determined. The data are the means ± SDs of three separate experiments. (D) Effect of human PDCD6 on HUVEC tube formation. Each transfectant was cultured on Growth Factor Reduced Matrigel, and then treated for 48 h with or without VEGF. The quantification of newly formed tubular structures was done from photographs taken using an inverted microscope. The tube lengths were quantified and are expressed as the mean ± SD. Three independent experiments were conducted in triplicate. *, $P<0.05$ compared with Mock.

siPDCD6, respectively. All-transfected cells were cultured in grown medium, cell viability was measured by using MTT assay system. These results indicate that PDCD6 strongly inhibited cell growth in various types of cancer cells (Fig. 3E).

As presented in Fig. 3A, PDCD6 markedly reduced the expression of HIF-α. This generally could be due to either a transcriptional effect or a stabilization effect on HIF-α that relates to modifying PHD2 function and ubiquitin-directed degradation. To explore the molecular mechanism between HIF-α and PHD2, cells were transfected with mock (an expression vector only without insert), PDCD6 or PDCD6 plus siPDCD6, respectively. PHD2 protein plays a pivotal role in regulating the HIF-α activity and enhances cell death. Here, PDCD6 increased protein expression of PHD2 in OVCAR-3 cells. Furthermore, knock-down PHD2 by using siRNA abrongated the decrease in HIF-α expression (Fig. 3F). These results indicate that PDCD6-induced translation of PHD2 is strongly modulated HIF-α expression.

Apoptosis-related pathways are activated downstream of the phosphoinositol 3-kinase, the activation of Akt, and p38/JNK, which two critical pathways involved in the regulation of cellular functions, were well-known. Akt is a serine/threonine kinase that is involved in modulating various biological responses, such as inhibition of apoptosis and induction of cell proliferation. p38/JNK plays a major role in regulation of proliferation in mammalian cells by sharing cellular substrate and interaction as well as involved in many physiological/pathological conditions, including cancer and other diseases. We then investigate the phosphorylation of p38/JNK in OVCAR-3 cells. As shown in Fig. 3G, p38/JNK phosphorylation was not inhibited by PDCD6. All of these results strongly indicate that PDCD6 can affect one or more steps within the Akt signaling pathway, depending on the complement of components that form the functional Akt signaling module.

3.3. Physically interaction of PDCD6 with VEGFR-2

To understand the molecular mechanism involved in the inhibition of angiogenesis by PDCD6, we used a yeast two-hybrid system and co-immunoprecipitation assay. We first checked the inhibitory effect of PDCD6 on VEGF-induced VEGFR-2 expression in HUVECs. The over-expression of PDCD6 specifically suppressed VEGFR-2 expression, whereas siPDCD6 did not affect (Fig. 4A). Positive interaction was

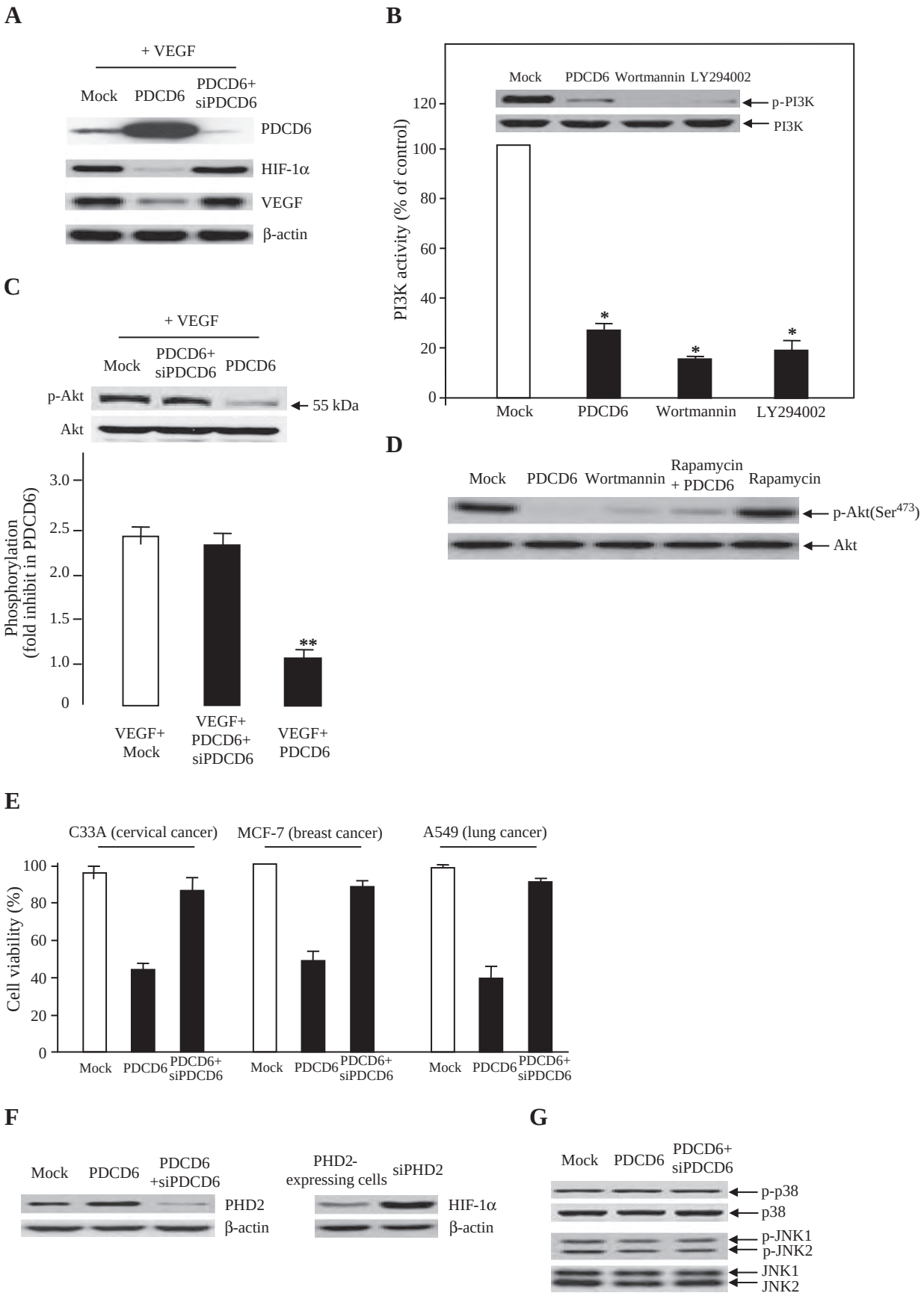
A
+ VEGF
Mock
PDCD6
PDCD6+ siPDCD6
PDCD6
HIF-1α
VEGF
β-actin
B
Mock
PDCD6
Wortmannin
LY294002
p-PI3K
PI3K
PI3K activity (% of control)
120
100
80
60
40
20
0
Mock
PDCD6
Wortmannin
LY294002
C
+ VEGF
Mock
PDCD6+ siPDCD6
PDCD6
p-Akt
Akt
55 kDa
Phosphorylation (fold inhibit in PDCD6)
3.0
2.5
2.0
1.5
1.0
0
VEGF+ Mock
VEGF+ PDCD6+ siPDCD6
VEGF+ PDCD6
D
Mock
PDCD6
Wortmannin
Rapamycin + PDCD6
Rapamycin
p-Akt(Ser473)
Akt
E
C33A (cervical cancer)
MCF-7 (breast cancer)
A549 (lung cancer)
Cell viability (%)
100
80
60
40
20
0
Mock
PDCD6
PDCD6+ siPDCD6
F
Mock
PDCD6
PDCD6 +siPDCD6
PHD2
β-actin
PHD2-expressing cells
siPHD2
HIF-1α
β-actin
G
Mock
PDCD6
PDCD6+ siPDCD6
p-p38
p38
p-JNK1
p-JNK2
JNK1
JNK2

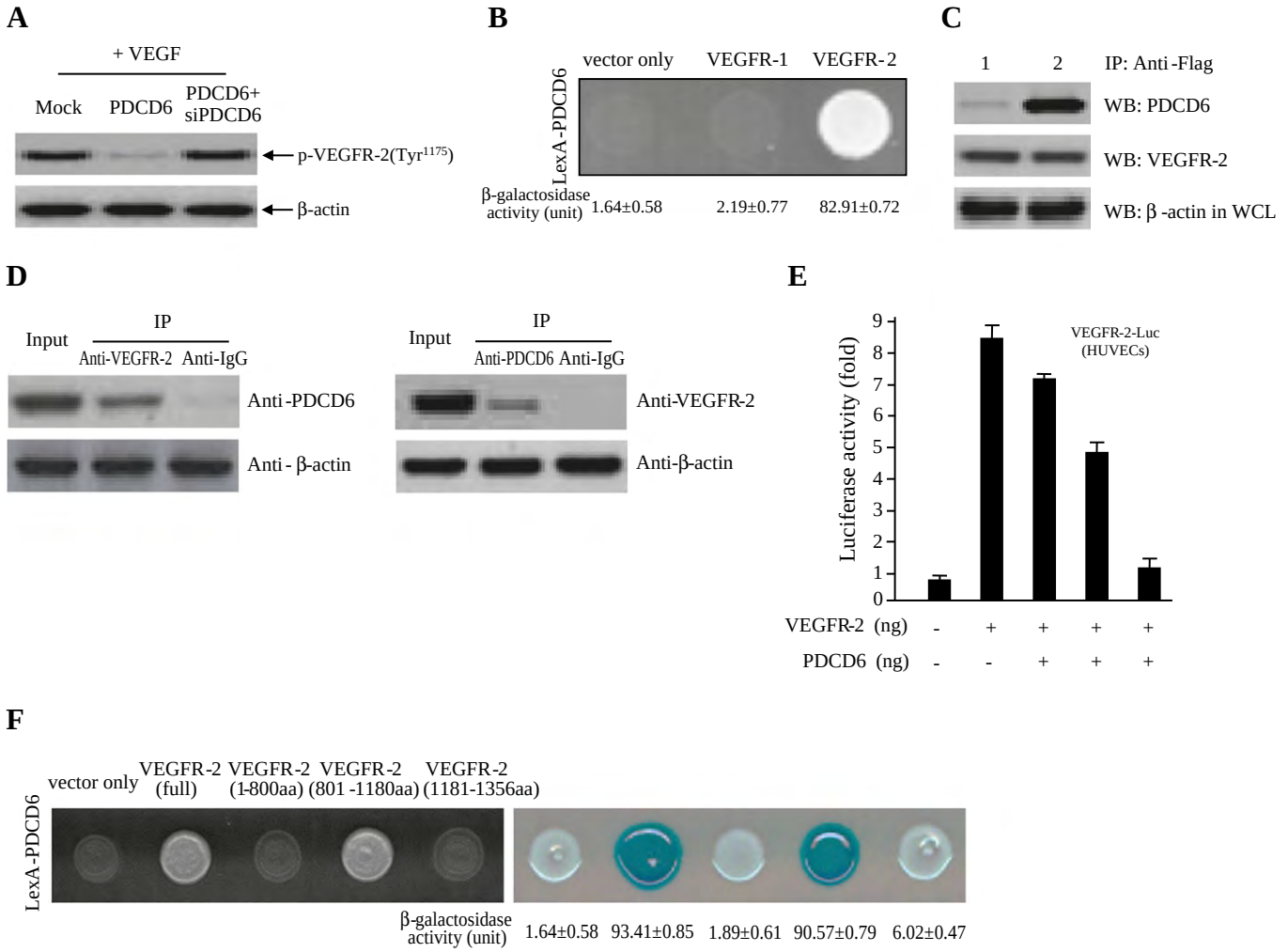

Fig. 4. Physical interaction between PDCD6 and VEGFR-2. (A) HUVECs were treated with VEGF and then mock-transfected or transfected with PDCD6 or PDCD6 plus siPDCD6. PDCD6 effectively inhibited the phosphorylation of VEGFR-2 triggered by VEGF. Phosphorylation of VEGFR-2 was determined by specific antibody. Actin was used for loading control. (B) Positive interactions were monitored by observing cell growth on medium lacking leucine, and by the formation of a blue colony on the X-gal plate. The values of β-galactosidase activity (unit) determined by adding *o*-nitrophenyl β-D-galactopyranoside (ONPG) assays are indicated below the corresponding lanes. (C) Co-immunoprecipitation of PDCD6 with VEGFR-2. Immunoprecipitation was performed using an anti-Flag antibody with lysates from both transfected HEK293 cells. After immunoprecipitation, precipitated proteins were immunoblotted using anti-PDCD6 and anti-VEGFR-2 antibody. *lane 1*, pcDNA3.1 (vector only) and pcDNA3.1/Flag-PDCD6 transfectant; *lane 2*, pcDNA3.1/Flag-PDCD6 and pcDNA3.1-VEGFR-2 transfectant. (D) Co-immunoprecipitation between the endogenous VEGFR-2 and PDCD6 displays the interactions of the two proteins. (E) Inhibition of VEGFR-2-dependent transcription by PDCD6. HUVEC cells were co-transfected with 500 ng of VEGFR-2-Luc, 500 ng of a VEGFR-2 expression plasmid (pcDNA3.1/VEGFR-2), and increasing concentrations of plasmid-encoding PDCD6 (pcDNA3.1/Flag-PDCD6) (50, 250, and 500 ng). (F) Mapping of the critical interaction region between PDCD6 and VEGFR-2 by using protein interaction system. The cDNA constructs were co-transformed into EGY48 yeast cells to test a protein–protein interaction within the yeast two-hybrid system. Positive interactions were revealed by observing cell growth (*left* panel), and by the formation of blue colony (*light* panel). The values of β-galactosidase activity in negative controls (vector only) of each construct were below 1.64 ± 0.58. Data are representative of three independent experiments and shown as means ± SD.

monitored by using both cell growth with leucin-deficient plate and ONPG β-galactosidase activity. VEGFR-1 was used as the negative control. As shown in Fig. 4B, the β-galactosidase activity between PDCD6 and VEGFR-2 was fully activated, but not with empty vector (vector only) and VEGFR-1. To further confirm the direct interaction between PDCD6 and VEGFR-2 that we monitored in the yeast two-hybrid assay, we examined by co-immunoprecipitation. Gene constructs of PDCD6 (pcDNA3.1/Flag-PDCD6) and VEGFR-2 (pcDNA3.1-VEGFR-2), or

Fig. 3. Effects of PDCD6 on PI3K activity, Akt phosphorylation, and p38/JNK phosphorylation in OVCAR-3 ovarian cancer cells. (A) OVCAR-3 cells were incubated with 10 ng/ml VEGF and then mock (vector only)-transfected or transfected with PDCD6 or PDCD6 plus siPDCD6. VEGF and HIF-1α expression was then assessed by Western blotting. Three independent experiments were conducted in triplicate. (B) OVCAR-3 cells were transfected with PDCD6 or PDCD6 plus siPDCD6, harvested, lysed, and measured using an in vitro PI3K assay. Mock (vector only)-transfected cultures served as controls. Box. Lysed OVCAR-3 cells were probed with anti-p85 polyclonal antibodies. PI3K was used to verify equal loading of the samples. The results are representative of three independent experiments. (C) p-Akt inhibition by mock (vector only), PDCD6, or PDCD6 plus siPDCD6 exposure in ovarian cancer cells. The expression of p-Akt and total Akt in cell lysates prepared from mock (vector only)-, PDCD6-, or PDCD6 plus siPDCD6-transfected OVCAR-3 cells were determined. (D) Comparison of inhibitory effects on p-Akt use either PI3K or mTOR inhibitor in OVCAR-3 cells. Equal amounts of cellular protein (20 μg) were subjected to SDS–PAGE, followed by Western blotting for Akt and p-Akt. Immunoblotting for unphosphorylated Akt was used as a loading control. Three independent experiments were assayed in triplicate. The values shown represent the means ± SD. *, $P<0.05$ and **, $P<0.01$ compared with Mock. (E) PDCD6 is critical for proliferation of human cancer cells. Decreased cell viability of siPDCD6 transfectant. C33A, MCF-7, and A549 cells were transfected with mock (an expression vector only without insert), PDCD6 or siPDCD6. All-transfected cells were cultured in grown medium, cell viability was measured by using MTT reduction. Each sample was assayed in triplicate and the bars represent the mean ± SD. (F) The effects of PDCD6 on the PHD2-mediated HIF-1α. The effect of PDCD6 on expression of PHD2 was determined (*left* panel). Changes in the HIF-1α protein by siPHD2 was measured by Western blotting (*light* panel). β-actin was used as a loading control. (G) Effects of PDCD6 on p38 and JNK1/2 phosphorylation. After transfection with PDCD6 or siPDCD6, the phosphorylation of MAP kinases was evaluated by immunoblotting. Immunoblotting for unphosphorylated p38 and JNK1/2 was used as a loading control. Three independent experiments were assayed in triplicate.

pcDNA3.1/Flag-PDCD6 and vector only (pcDNA3.1) were co-transfected into HEK293 cells. Subsequently, an immunoprecipitation was subjected using anti-Flag antibody with lysates from both transfected cells. After immunoprecipitation, the precipitated proteins were immunoblotted using anti-PDCD6 or anti-VEGFR-2 antibody. In Fig. 4C, pcDNA3.1-VEGFR-2 was co-immunoprecipitated with pcDNA3.1/Flag-PDCD6 (*lane 2* in *upper* panel), whereas not with pcDNA3.1 (vector only) (*lane 1* in *upper* panel). We then investigated the interaction between endogenous PDCD6 and VEGFR-2 (Fig. 4D).

To address whether how PDCD6 regulates VEGFR-2, the effect of PDCD6 on the VEGFR-2 transcription was also examined by a luciferase reporter assay, using a construct introducing VEGFR-2 promoter fused to the luciferase gene. The luciferase activity was inhibited by the transfection of PDCD6 in a dose-dependent manner (Fig. 4E), further supporting the importance of PDCD6 for the control of VEGFR-2 activity. Our results suggest that over-expression of PDCD suppresses its transcriptional activity.

To identify the PDCD6 binding region of VEGFR-2, cDNA constructs containing three VEGFR-2 deletion mutants were designed as shown in Fig. 4F. In the two-hybrid system, the full-length human PDCD6 cDNA and either plasmid containing a full-length human VEGFR-2 or plasmids containing three truncation mutant forms (Met^{1}-Gly^{800}, Tyr^{801}-Ile^{1180}, Ser^{1181}-Val^{1356}) of cDNAs were co-transformed into EGY48 yeast cells. Cells containing full-length VEGFR-2 cDNA and also one deletion mutant (Tyr^{801}-Ile^{1180}) grew on the Ura, His, Trp and Leu deficient plates. Yeast cells transformed with the other deletion mutants (Met^{1}-Gly^{800} and Tyr^{801}-Ile^{1180}) failed to grow (Fig. 4F, *left* panel). To confirm this result, we quantitated the binding activity of these constructs by measuring the relative expression level of β-galactosidase. As shown in *right* panel in Fig. 4F, β-galactosidase assay results indicated that the critical VEGFR-2 region for binding PDCD6 resided within Tyr^{801}-Ile^{1180}. Collectively, our results strongly indicated that PDCD6 directly interacts with VEGFR-2 in cellular physiological condition.

3.4. PDCD6 suppress the phosphorylation of PI3K/mTOR/p70S6K pathway in endothelial cells

Interaction between VEGF and VEGFR-2 plays an important role in the activation of major downstream effectors responsible for proliferation, including endothelial cell migration, differentiation, survival as well as embryonic angiogenesis [16–18]. To further explore the functional mechanism underlying the anti-angiogenic effects of PDCD6, we investigated the effect on the levels of downstream signaling cascade components in the Akt pathway that control the endothelial cell function for the inhibition of angiogenesis. PDCD6 inhibited VEGF-induced phosphorylation of Akt signaling pathway, including mammalian target of rapamycin (mTOR), tuberous sclerosis complex 2 (TSC-2), p70 ribosomal protein S6 kinase (p70S6K), and glycogen synthase kinase-3β (GSK-3β) and effectively decreased the expression of cyclin D1, whereas VEGF-induced mitogen-activated protein kinase/extracellular signal-regulated kinase kinases (MEK1/2) and extracellular signal-regulated kinases (ERK1/2) phosphorylation were not suppressed by PDCD6 (Fig. 5). Thus, it shows that PDCD6 inhibits the PI3K/mTOR/p70S6K signaling pathway in HUVECs (data not shown) or OVCAR-3 ovarian cancer cells.

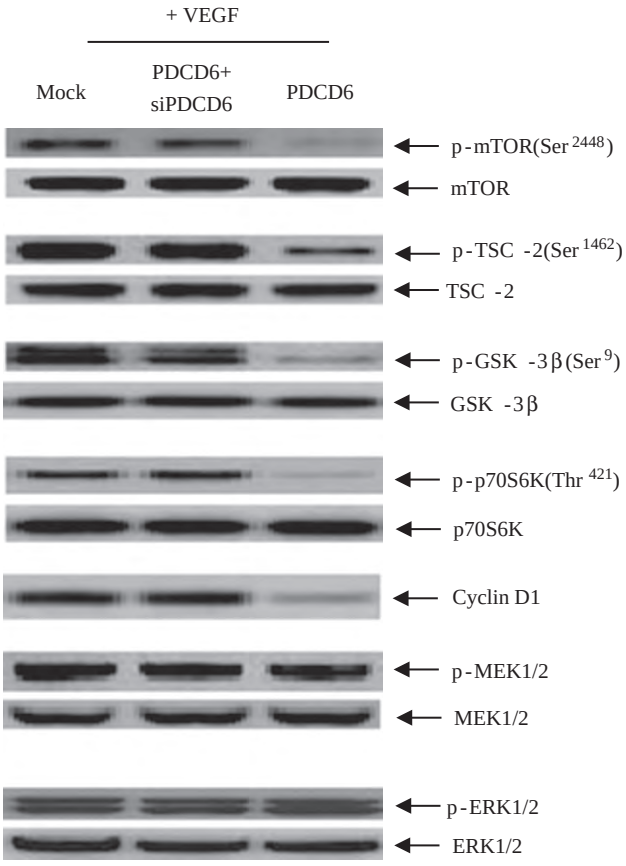

Fig. 5. PDCD6 suppressed the phosphorylation of downstream effectors in the PI3K/mTOR/p70S6K signaling pathways. After transfection with OVCAR-3 or HUVECs, cells were harvested for Western blot analysis with antibodies specific for phosphorylated or non-phosphorylated proteins indicated for mTOR phosphorylation, and the phosphorylation of downstream effectors, including tuberous sclerosis complex 2 (TSC-2), p70 ribosomal protein S6 kinase (p70S6K), glycogen synthase kinase-3β (GSK-3β), mitogen-activated protein kinase/extracellular signal-regulated kinase kinases (MEK1/2), and extracellular signal-regulated kinases (ERK1/2).

4. Discussion

In the present report, we demonstrated that a new critical molecular mechanism of PDCD6, as a novel potent anti-angiogenic factor can target the PI3K/Akt signaling pathway. PDCD6 plays a pivotal positive role in apoptosis and facilitates anti-tumor activity in ovarian cells. Cancerous tumors that have become metastatic are malignant and do not possess normal cells. These tumors grow over time, consume surrounding tissue, and eventually metastasize. In contrast, growth and apoptosis in normal cells are in equilibrium. During cancer progression, the uncontrolled rates of cell proliferation and cell death have important physiological roles, leading to invasion and angiogenesis. Tumor angiogenetic cells may also arise from increased growth due to anti-apoptotic factors or mutations in tumor suppressor genes [19–21]. Previous studies have reported the increased expression of PDCD6 in some cancers, including small-cell lung cancer [11]. Recently, la Cour et al. [22] reported the expression of PDCD6 in tumor tissue samples of various cancer types as well as in normal samples. Most notably, clinical and experimental studies have found that PDCD6 is up-regulated in mesenchymal tumors.

Angiogenesis is essential in early development, tissue repair, inflammatory disease, and tumor metastasis. This complex process, which includes the regulation of endothelial cell proliferation, migration, invasion, and the formation of new lumen vessels from pre-existing vessels, is a key step in tumor growth [23,24] and progression, as it enables a supply of nutrients and oxygen to fuel tumor growth [25]. VEGF, a key regulator of blood vessel formation during organ development, induces the proliferation and migration of endothelial cells [24]. In tumors, endothelial cell activity plays a crucial role in regulating various vascular physiological functions and diseases. Although VEGFR-1 and VEGFR-2 are structurally very similar, but have divergent effects on angiogenesis. VEGFR-2 plays an important role to the activation of major downstream effectors responsible for proliferation, including endothelial cell migration, differentiation, survival as well as embryonic angiogenesis [16–18], whereas VEGFR-1 is not associated with proliferation of endothelial cells [26].

In this study, we further investigated the possible contribution of PDCD6 to angiogenesis using HUVECs to assay proliferation, migration, invasion, and tube formation and found that PDCD6 facilitates these processes in HUVECs.

Recent studies have suggested that PI3K suppression may play an important role in tumor angiogenesis [27–29]. PI3K mediates signaling pathways involved in cell death, growth, or both. In apoptosis, the anti-apoptotic signal mediated by Akt protein kinase begins at PI3K. Akt is a major downstream target of PI3K in the angiogenic pathway. Akt regulates tumor angiogenesis, cell cycle progression, and cell proliferation, migration, metabolism, and survival [30,31]. In animal studies, the siRNA-mediated inhibition of Akt effectively reduced ovarian tumor growth and angiogenesis [27,29]. The PI3K/Akt signaling pathway plays an important role in tumor angiogenesis. mTOR is critical in the control of cell growth and proliferation, and mediate their signals in various signaling pathways [32,33]. In this study, PDCD6 inhibited VEGF-induced phosphorylation of Akt signaling pathway, including mammalian target of rapamycin (mTOR), tuberous sclerosis complex 2 (TSC-2), p70 ribosomal protein S6 kinase (p70S6K), and glycogen synthase kinase-3β (GSK-3β) and effectively decreased the expression of cyclin D1, whereas VEGF-induced mitogen-activated protein kinase/extracellular signal-regulated kinase kinases (MEK1/2) and extracellular signal-regulated kinases (ERK1/2) phosphorylation were not suppressed by PDCD6. In addition, we next show complete G_0–G_1 phase cell arrest in OVCAR-3 ovarian cancer cells after PDCD6 transiently transfection, whereas it did not suppress phosphorylation of either MEK1/2 or ERK1/2, suggesting that PDCD6 does not suppress signal components in the Ras-ERK signaling pathway. We believe this anti-angiogenic activity stems mainly from the anti-proliferative and -migratory effect of PDCD6 on endothelial cells, given the importance of PI3K/Akt signaling in endothelial cell invasion and growth.

In conclusion, genetic and molecular manipulations have identified PDCD6 as an important mediator of tumor angiogenesis. These findings strongly suggest that PDCD6 can inhibit tumor growth via suppression of tumor angiogenesis in the cellular physiological condition through targeting PI3K/mTOR/p70S6K kinase signaling pathway. Importantly, our study is the first to show that PDCD6 is involved in angiogenesis and provides a potential molecular target for the treatment of certain malignant tumors.

Acknowledgments

We thank Dr. S.A. Martinis (Department of Biochemistry, University of Illinois at Urbana-Champaign, IL, USA), and Richard Yoo (University of Washington, Seattle, WA, USA) for critical reading of the manuscript. This work was supported by a grant from the National Cancer Center, Korea (NCC-0910262-3).

Appendix A. Supplementary data

Supplementary data to this article can be found online at doi:10.1016/j.cellsig.2011.08.013.

References

[1] P. Vito, E. Lacana, L. D'Adamio, Science 271 (1996) 521–525.
[2] J. Krebs, P. Saremaslani, R. Caduff, Biochimica et Biophysica Acta 1600 (2002) 68–73.
[3] M. Missotten, A. Nochols, K. Rieger, R. Sadoul Alix, Cell Death and Differentiation 6 (1999) 124–129.
[4] H. Suzuki, M. Kawasaki, T. Inuzuka, M. Okumura, T. Kakiuchi, H. Shibata, S. Wakatsuki, M. Maki, Structure 16 (2008) 1562–1573.
[5] Y.S. Jung, K.S. Kim, K.D. Kim, J.S. Lim, J.W. Kim, E. Kim, Biochemical and Biophysical Research Communications 288 (2001) 420–426.
[6] H. Satoh, H. Shibata, Y. Nakano, Y. Kitaura, M. Maki, Biochemical and Biophysical Research Communications 291 (2002) 1166–1172.
[7] J.H. Lee, S.B. Rho, T. Chun, Biotechnology Letters 27 (2005) 1011–1015.
[8] K. Katoh, H. Suzuki, Y. Terasawa, T. Mizuno, J. Yasuda, H. Shibata, M. Maki, Biochemical Journal 391 (2005) 677–685.
[9] A. Yamasaki, K. Tani, A. Yamamoto, N. Kitamura, M. Komada, Molecular Biology of the Cell 17 (2006) 4876–4887.
[10] H. Shibata, H. Suzuki, T. Kakiuchi, T. Inuzuka, H. Yoshida, T. Mizuno, M.M. Maki, Journal of Biological Chemistry 283 (2008) 9623–9632.
[11] J.M. la Cour, J. Mollerup, P. Winding, S. Tarabykina, M. Sehested, M.W. Berchtold, American Journal of Pathology 163 (2003) 81–89.
[12] Y. Yamada, T. Arao, T. Gotoda, H. Taniguchi, I. Oda, K. Shirao, Y. Shimada, T. Hamaguchi, K. Kato, T. Hamano, F. Koizumi, T. Tamura, D. Saito, T. Shimoda, M. Saka, T. Fukagawa, H. Katai, T. Sano, M. Sasako, K. Nishio, Cancer Science 99 (2008) 2193–2199.
[13] O.H. Lee, Y.M. Kim, Y.M. Lee, E.J. Moon, D.J. Lee, J.H. Kim, K.W. Kim, Y.G. Kwon, Biochemical and Biophysical Research Communications 264 (1999) 743–750.
[14] S.B. Rho, K.H. Lee, J.W. Kim, K. Shiba, Y.J. Jo, S. Kim, Proceedings of the National Academy of Sciences of the United States of America 93 (1996) 10128–10133.
[15] K.H. Plate, G. Breier, H.A. Weich, W. Risau, Nature 359 (1992) 845–848.
[16] G. Breier, Advances in Experimental Medicine and Biology 476 (2000) 57–66.
[17] N. Ferrara, American Journal of Physiology. Cell Physiology 280 (2000) C1358–C1366.
[18] R.D. Meyer, N. Rahimi, Annals of the New York Academy of Sciences 995 (2003) 200–207.
[19] D.R. Green, G.I. Evan, Cancer Cell 1 (2002) 19–30.
[20] M.S. Soengas, P. Capodieci, D. Polsky, J. Mora, M. Esteller, X. Opitz-Araya, R. McCombie, J.G. Herman, W.L. Gerald, Y.A. Lazebnik, S.W. Cordon-Cardo, Nature 409 (2001) 207–211.
[21] L. Subramanian, J.W. Crabb, J. Cox, I. Durussel, T.M. Walker, P.R. van Ginkel, S. Bhattacharya, J.M. Dellaria, K. Palczewski, A.S. Polans, Biochemistry 43 (2004) 11175–11186.
[22] J.M. la Cour, B.R. Høj, J. Mollerup, R. Simon, G. Sauter, M.W. Berchtold, Molecular Oncology 1 (2008) 431–439.
[23] J. Folkman, Y. Shing, Journal of Biological Chemistry 267 (1992) 10931–10934.
[24] W. Risau, Nature 386 (1997) 671–674.
[25] G.D. Yancopoulos, S. Davis, N.W. Gale, J.S. Rudge, S.J. Wiegand, J. Holash, Nature 407 (2000) 242–248.
[26] R.D. Meyer, A. Singh, F. Majnoun, C. Latz, K. Lashkari, N. Rahimi, Oncogene 23 (2004) 5523–5531.
[27] C. Xia, Q. Meng, Z. Cao, X. Shi, B.H. Jiang, Journal of Cellular Physiology 209 (2006) 56–66.
[28] J.L. Arbiser, T. Kau, M. Konar, K. Narra, R. Ramchandran, S.A. Summers, C.J. Vlahos, K. Ye, B.N. Perry, W. Matter, A. Fischl, J. Cook, P.A. Silver, J. Bain, P. Cohen, D. Whitmire, S. Furness, B. Govindarajan, J.P. Bowen, Blood 109 (2007) 560–565.
[29] B.H. Jiang, L.Z. Liu, Biochimica et Biophysica Acta 1784 (2008) 150–158.
[30] V. Duronio, M.P. Scheid, S. Ettinger, Cellular Signalling 10 (1998) 233–239.
[31] B.H. Jiang, J.Z. Zheng, P.K. Aoki, Proceedings of the National Academy of Sciences of the United States of America 97 (2000) 1749–1753.
[32] D.C. Fingar, S. Salama, C. Tsou, E. Harlow, J. Blenis, Genes & Development 16 (2002) 1472–1487.
[33] X. Wan, B. Harkavy, N. Shen, P. Grohar, L.J. Helman, Oncogene 26 (2007) 1932–1940.